PALAIOS
Emphasizing the impact of life on Earth's history

PALAIOS, 2014, v. 29, 233–249
Research Article
DOI: http://dx.doi.org/10.2110/palo.2013.049

1926 SEPM Society for Sedimentary Geology

MICROBIALITES IN A HIGH-ALTITUDE ANDEAN LAKE: MULTIPLE CONTROLS ON CARBONATE PRECIPITATION AND LAMINA ACCRETION

FERNANDO J. GOMEZ,[1] LINDA C. KAH,[2] JULIE K. BARTLEY,[3] AND RICARDO A. ASTINI[1]
[1]*LAC-Laboratorio de Análisis de Cuencas, CICTERRA (CONICET-UNC) Centro de Investigaciones en Ciencias de la Tierra, FCEFyN-Universidad Nacional de Córdoba, (Córdoba) Argentina, fgomez@cicterra-conicet.gov.ar, raastini@efn.uncor.edu*
[2]*Department of Earth and Planetary Sciences, University of Tennessee, Knoxville, Tennessee, USA, lckah@utk.edu*
[3]*Geology Department, Gustavus Adolphus College, Minnesota, USA, jbartley@gustavus.edu*
e-mail: fgomez@cicterra-conicet.gov.ar

ABSTRACT: **Microbialites comprise the mineralized record of early life on Earth and preserve a spectrum of fabrics that reflect complex physical, chemical, and biological interactions. The relatively rarity of microbialites in modern environments, however, challenges our interpretation of ancient structures. Here we report the occurrence of microbial mats, mineral precipitates, and oncoids in the Laguna Negra, a high-altitude hypersaline Andean lake in Catamarca Province, Argentina. Laguna Negra is a Ca-Na-Cl brine where abundant carbonate precipitation takes place. Extreme environmental conditions, including high UV radiation, elevated salinity, and temperature extremes, restrict multicellular life so that mineralization reflects a combination of local hydrologic conditions, lake geochemistry, and microbial activity. The resulting carbonates consist of micritic laminae, botryoidal cement fans, and isopachous cement laminae that are strikingly similar to those observed in Proterozoic stromatolites, providing insight into mechanisms of mineralization. Here, increased saturation with respect to carbonate minerals reflects mixing of spring-fed inlets and lake waters, favoring microbialite formation and preservation. This highlights the importance of hydrological mixing zones in microbialite formation and as taphonomic windows to record microbial activity. Recent discoveries of minerals related to evaporating playa-lake systems on Mars further highlights the potential of Laguna Negra to provide critical insight into biosignature preservation in both terrestrial and extraterrestrial settings.**

INTRODUCTION

Microbialites (Burne and Moore 1987) result from a complex interplay of microbial growth and decomposition combined with mineral precipitation and sediment deposition (Grotzinger and Knoll 1999; Reid et al. 2000, Dupraz and Visscher 2005). Modern laminated microbialites, known as stromatolites (Kalkowski 1908; Walter 1972), often have macroscopic morphologies similar to their Proterozoic counterparts; however, their microstructures are strikingly different, making many modern stromatolites a poor analogue for Proterozoic structures (Kempe and Kazmierczac 2006) and limiting our ability to interpret the conditions under which Proterozoic stromatolites formed.

Although usually considered organosedimentary structures (Burne and Moore 1987), stromatolitic morphologies may also form without clear biological control (Grotzinger and Rothman 1996; Grotzinger and Knoll 1999; Cuerno et al. 2012). The distinction between biotic and abiotic control of stromatolite formation is not trivial; stromatolites are generally considered among the oldest evidence for life on Earth (Allwood et al. 2006). In addition, stromatolites have been considered as a critical indicator in the astrobiological search for habitable environments (Summons et al. 2011). Unfortunately, determination of primary biotic (or abiotic) signatures in geological ancient deposits is oftentimes hampered by taphonomic and geochemical changes that occur during postdepositional diagenesis. In the absence of preserved mat components or geochemical characteristics uniquely attributable to biological activity, lamina-scale microfabrics may provide key links between process and product in stromatolite genesis (cf. Reid et al. 2000; Visscher et al. 2000). Additionally, the investigation of modern analogues, where biochemical processes can be directly observed and where secondary alteration processes are largely absent, is critical to our identification and differentiation of biotically and abiotically controlled signatures.

Microbialites in Laguna Negra, Catamarca Province, Argentina, preserve a range of microfabrics comparable to those observed in Proterozoic stromatolites. Extremes in ultra violet (UV) radiation, temperature, and chemical activity in this high-altitude (~ 4500 m), hypersaline lake (Table 1) restrict the occurrence of nonmicrobial elements, favoring direct precipitation of mineral components on and within the microbial mat substrate developed in groundwater spring-fed pools. Furthermore, characteristic mat fabrics are arrayed spatially along hydrologic, chemical, and microbial gradients that shed light on both the mechanisms of fabric development in stromatolites and the range of environmental conditions that are most favorable to recording microbial activity. Combined, these features suggest that Laguna Negra has much to offer as an analogue for ancient terrestrial (Buick 1992; Awramik and Buchheim 2009) and, potentially, extraterrestrial environments.

To our knowledge, no previous description of Laguna Negra has been published and this is the first report of carbonate microbialites in lakes within Catamarca Province, Argentina. Modern stromatolites have been described by Farías et al. (2011) for Socompa and Tolar Grande (Salta and Jujuy provinces, Argentina, respectively) and similar modern and recent (Holocene) microbialites have also been described by Risacher and Eugster (1979), Jones and Renault (1994), Rouchy et al. (1996) and

Published Online: September 2014
 0883-1351/14/029-233/$03.00

TABLE 1.—*Environmental parameters in the region of the Laguna Verde Complex.*

Parameter	Value	References
Altitude	~4500 m	Altimeter and GPS values
Atmospheric pressure	615–650 mbars	Pascua Lama-Veladero Project Meteorological data[1]
Precipitation rate	≤100–250 mm/year	Valero-Garces et al., 2000; Boschetti et al., 2007
Evaporation rate	1200–1500 mm/y	Valero-Garces et al., 2000; Boschetti et al., 2007
Relative humidity	15–20% (at 600 mbar)	Boschetti et al., 2007
Summer Temperature range	+30 C to −10 C	Pascua Lama-Veladero Project Meteorological data[1]
Winter Temperature range	+8 C to −30 C	Pascua Lama-Veladero Project Meteorological data[1]
Precipitation as snow	50–80%	Vuille and Amman, 1996; Valero-Garces et al., 2000
Maximum Wind velocity	443.2 Km/h	Milana, 2009
Wind direction	From NW to SE	Milana, 2009
UV-B (200–315 nm) influx	10.8 W/m^2	Fernandez-Zenoff et al., 2006; Farias et al., 2011

[1] http://mineria.sanjuan.gov.ar/index.php.

Valero-Garcés et al. (1999, 2000) for the Altiplano-Puna region of Chile and Bolivia. Although such terms as pisoids (Risacher and Eugster 1979; Jones and Renault 1994), dendroidal oncolites (Wade and García Pichel 2003) and stromatolitic oncoids (Garcia-Pichel et al. 2004) have been used for similar structures, here we refer to them generally as oncoids, although this term does not always reflect the morphological complexity of these structures.

The main purpose of this work is to describe previously unreported lacustrine microbialites and their environmental setting within Laguna Negra and to interpret mechanisms of lamina accretion. Because Laguna Negra microbialites preserve a range of microfabrics remarkably similar to those observed in Proterozoic stromatolites, we expect that these data will permit us to evaluate the potential of Laguna Negra to inform interpretations of Precambrian microfabric development and to discuss implications for astrobiological research.

GEOLOGICAL SETTING AND CLIMATE

Laguna Negra (GPS 27°38′49″ S, 68°32′43″ W) is located at the southeast end of the Laguna Verde Complex (LVC), in the southernmost Puna region of Catamarca Province, Argentina (Fig. 1). The Puna consists of a high-altitude plateau (average altitude ~ 3700 m) dominated by andesitic to basaltic volcanic rocks with minor rhyolite, dacite, and ignimbrite. Intermontane basins, separated by north-south trending mountain ranges (with peaks > 6000 m), formed in the Cenozoic. Thick successions of siliciclastic and evaporite strata record rapid Cenozoic uplift (Jordan and Alonso 1987) and progressive environmental restriction (Vandervoort et al. 1995). The LVC consists of a series of lakes and salars resulting from progressive geographical isolation (Vandervoort et al. 1995) and increased aridity since the last glacial maximum (Valero-Garcés et al. 2000). Unlike the well-known salars of the Chilean Atacama (Risacher et al. 2003 and references therein), the lakes of the Argentinian Puna remain relatively unstudied and, to our knowledge, this is the first contribution focused on this particular area.

Laguna Negra (Figs. 1, 2) is a shallow (< 2 m) hypersaline lake with an area of ~ 8.63 km^2 and a strongly negative water balance (Table 1). Silty to sandy, immature siliciclastic sediment covers part of the present lake area. Mineral precipitation in Laguna Negra consists of both evaporite (halite, polyhalite, and gypsum) and carbonate (calcite and minor aragonite) lithologies. An extensive salt flat comprises more than 50% of the lake basin (Figs. 1, 2), and effectively isolates Laguna Negra from the rest of the LVC. Evaporite precipitation is readily triggered by temperature and wind-driven evaporation of surface water. Open water occurs exclusively in the southern portion of the lake, where water enters intermittently via surface drainage of seasonal to perennial snowpack and marginal groundwater seeps.

Carbonate deposits are restricted to the southeastern edge of Laguna Negra and consist of oncoids and laminar mineralized crusts that occur within a broad (0.3 km^2), shallow-water (< 10 cm) margin constructed by the northward progradation of alluvial fans (Fig. 3; herein referred to as the stromatolite belt). The stromatolite belt consists of three distinct zones: Zone 1: a proximal belt that is colonized by salt-marsh grass, *Spartina* sp., which delineates regions of freshwater input; Zone 2: an intermediate zone consisting of microbial ponds that lack both oncolitic structures and mineralization; and Zone 3: the main belt of carbonate microbialites and crusts. Zone 3 contains subzones defined by a combination of microbialite morphology, water depth, and salinity: laminar mineralized crusts predominate in Zone 3A (Fig. 3); cm-scale, carbonate gravels and gravel aggregates dominate Zone 3B (Fig. 3); oncoids are concentrated primarily within Zone 3C (Fig. 3); and Zone 3D is represented primarily by peloidal to micritic carbonate sediment, locally interlayered with gypsum or organic-rich laminae (Fig. 3). The current study focuses on microbialite structures and laminar crusts found primarily within zones 3A and 3C, which represent the majority of the stromatolite belt.

METHODS

Environmental and Climate Data

There are currently no meteorological stations in the region of the Laguna Verde Complex, and the climatic information for the Puna region is limited; Table 1 provides meteorological and environmental data reported from the Pascua Lama-Veladero mining district, which lies ~ 230 km to the southwest of (and at a comparable altitude to) the Laguna Verde Complex, as well as data reported from elsewhere in the Puna region (Fernandez-Zenoff et al. 2006; Ordoñez et al. 2009; Farías et al. 2011). A meteorological station has been acquired and will be installed at Laguna Negra in 2014, as part of an ongoing environmental monitoring project. Extreme environmental conditions typically restrict fieldwork to mid-spring through early fall, between late October and early April.

Lake Water Chemistry

Preliminary chemical assessment of inlet and lake waters is reported in Table 2. Field sampling was carried out in January 2009, with water sample locations selected to provide a compositional overview of lake, inlet, and mixing zone waters. For comparison, an additional sample was taken from Laguna Verde, which lies north of Laguna Negra and is isolated from Laguna Negra by an extensive salt flat.

In situ analyses were made using a HACH Saltwater Aquaculture Test Kit (Model FF-3) following procedures specified in the manufacturer's manual. Salinity and pH measured by titration with mercuric chloride were in good agreement with duplicate measurements using conductivity

FIG. 1.—Location map (upper right) and satellite image of the Laguna Verde Complex (LVC), showing Laguna Negra, the focus of this study. The LVC is 36 km long, measured along the major axis. Laguna Negra major and minor axes are 7.5 × 4 km, respectively.

FIG. 2.—Panoramic view of Laguna Negra, with the saline plain, the main lake, and the stromatolite belt where carbonate precipitation and microbial mats are located.

and pH probes. CO_2 was determined in 100 mL samples by titration with sodium hydroxide to the phenolphthalein end point (and expressed in mg/L). Alkalinity was determined *in situ* by titration immediately after sampling, is expressed as Total Alkalinity (carbonate, bicarbonate, and hydroxide alkalinity), and reported in mg/L of equivalent calcium carbonate. Hardness (i.e., the total calcium plus magnesium concentration) was determined by titration to a pH of 10.1 (using a Hardness 1 Buffer solution) followed by titration with EDTA to a blue end point, expressed in mg/L of equivalent calcium carbonate.

Additional analyses of dissolved species were performed at the University of West Georgia. Cation concentration was measured using a PerkinElmer ICP-OES fitted with a Meinhardt concentric nebulizer and calibrated to a series of gravimetrically determined standards. Anion concentrations were performed on a Thermo Scientific Dionex Ion

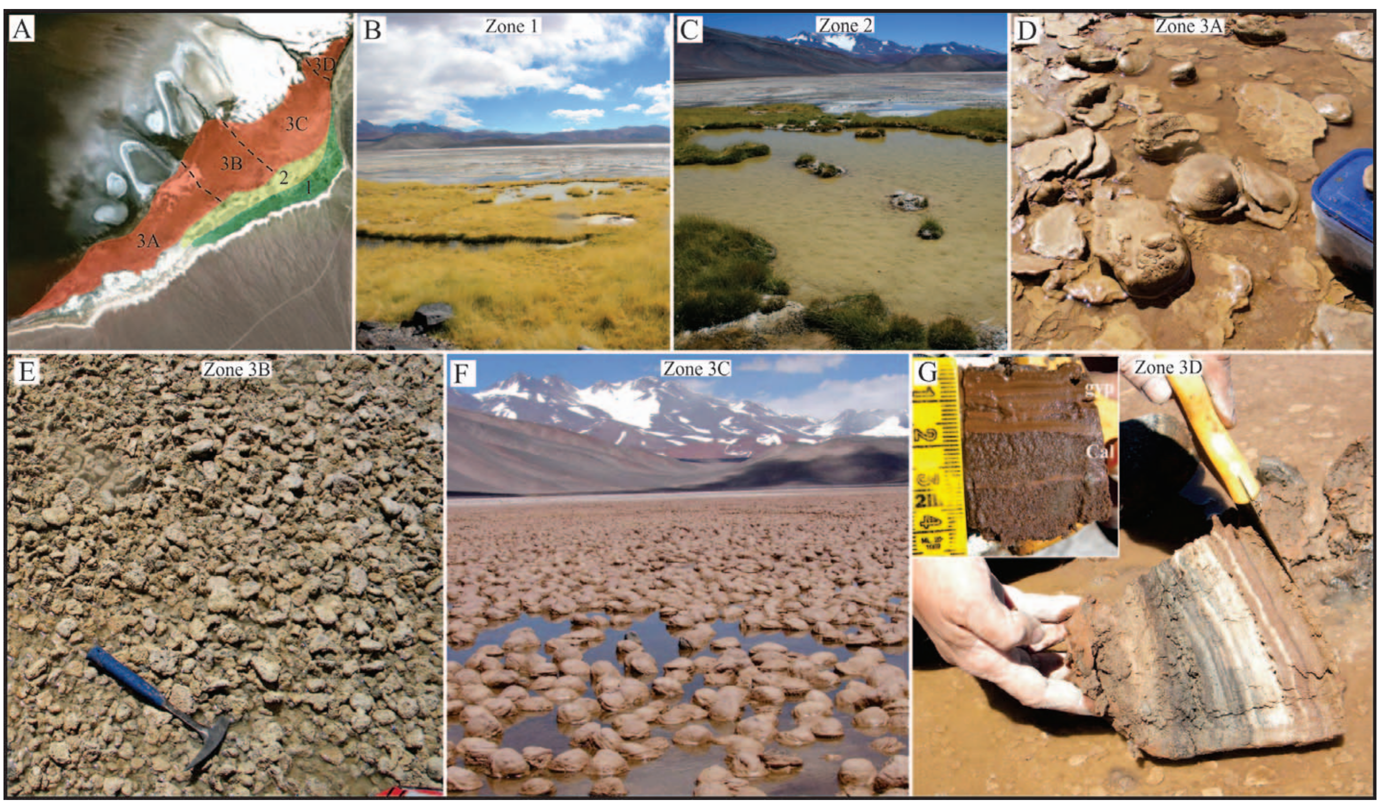

FIG. 3.—**A**) Satellite image (upper left) of Laguna Negra, showing the spatial distribution of the microbialites and related mineral precipitates. **B**) Zone 1: proximal belt colonized by salt-marsh grass. **C**) Zone 2: an intermediate zone with microbial ponds but without stromatolite-like structures, bordered by salt-marsh grass. **D–G**) Zone 3: the stromatolite belt (SB), which also shows subzones. **D**) Laminar crusts predominate in Zone 3A. **E**) Cm-size gravel-like carbonate aggregates are located in Zone 3B. **F**) Oncoids typically seen in Zone 3C. **G**) Zone 3D is mostly represented by peloidal to micritic carbonate sediments, locally interlayered with gypsum (see inset) or discontinuous organic-rich beds. The present work focuses mainly on structures occurring in Zones 3A and 3C.

TABLE 2.—*Laguna Negra water chemistry. LW and IW represent average lake water and inlet water, respectively. These values are used for geochemical modeling (salinity reported in ppt; all others in mg/L).*

Sample	Description	pH	CO_2 mg/L	Temp. (Celsius)	Salinity ppt	Hardness mg/L	Alkalinity mg/L	Na^+ mg/L	K^+ mg/L	Mg^{+2} mg/L	Ca^{+2} mg/L	Cl^- mg/L	SO_4^{-2} mg/L
1	Lake water	5.7	2886.4	18.5	324.8	10900	880	61921	3998	5180	14650	196100	82
2	Lake water	5.61	3520	15.7	316.8	n.d.	930	61562	5320	7180	14650	204800	95
3	Mixing zone	7.71	231.2	21.7	16.3	12800	550	2969	293	400	330	75200	128
4	Mixing zone	6.5	982	20.8	120	38100	300	28894	1328	2150	6120	68800	176
5	Laguna Verde	6.01	1816.3	10.9	246.8	66200	600	56204	2320	1860	14780	144600	114
6	Inlet water	7.87	214.7	20.8	15.4	5300	290	2845	158	450	820	9450	30.9
7	Inlet water	7.84	218.2	20	9.1	2000	430	876	146	260	460	5630	21.7
8	Inlet water	7.46	288.6	22.8	27.4	6600	200	6638	379	1230	2630	19990	495
9	Inlet water	7.52	285.1	23.1	22.1	5300	160	4154	178	970	1910	13780	322
10	Lake water	5.84	2601.3	6.8	285.6	90000	690	90922	7420	7680	19280	198100	108
11	Inlet water	5.7	2562.6	31.1	316.4	83900	330	143726	6216	6640	19210	208400	104
12	Inlet water	6.88	423.96	31.6	62.8	24000	40	6903	258	1590	5740	38830	506
LW	Average Lake Water (n=3)	5.7	3002.5	–	309	–	833.3	71468.3	5579.33	6680	16193.3	199666	95
IW	Average Inlet Water (n=4)	7.7	215.65	–	18.5	–	270	3628.25	215.25	727.5	1455	12212.5	217.3

Chromatograph. Reproducibility for all ions is better than 10%, based on replicate measurements of sample and standard solutions.

Mineralogical and Petrographic Analyses

Mineralogical composition of microbialite and sediment samples were identified via X-ray diffraction using a Philips X'PERT PRO diffractometer housed within the Departamento de Cristaloquímica de la Facultad de Ciencias Químicas, Universidad de Cordoba. Petrographic analysis of microfabrics was carried out at the University of Tennessee using standard polarized light microscopy equipped with epifluorescence (wideband blue and UV) capabilities. Petrographic analyses were augmented by scanning electron microscopy carried out at the Laboratorio de Microscopía Electrónica y Microanalísis, Universidad de Cordoba; and at the Universidad de San Luis.

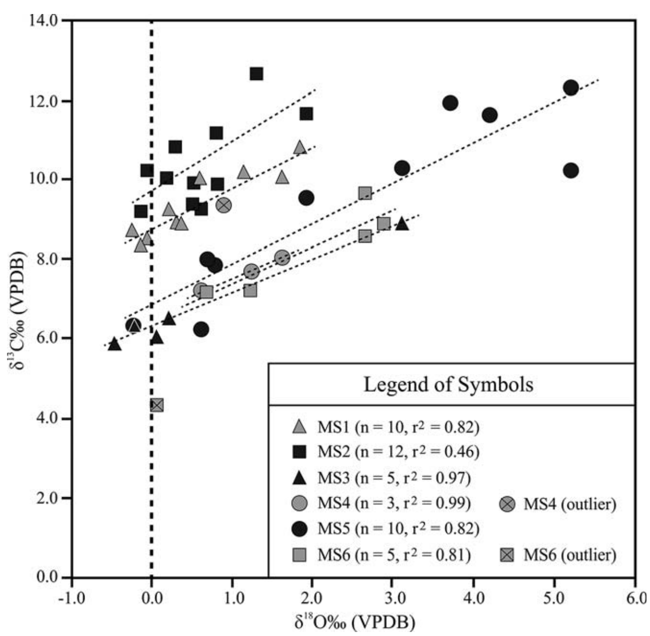

FIG. 4.—Stable isotope ($\delta^{13}C$ and $\delta^{18}O$) cross-plot of the Laguna Negra carbonates. MS1 to MS6 represent different samples including laminar crusts and Oncoids that were sampled by microdrilling of individual laminae, from the core to the edge of the structures. The values marked as outliers were not included in the calculation of the trendline.

Isotopic Analyses

Analysis of stable carbon and oxygen isotopes of Laguna Negra microbialites was performed at the University of Tennessee; results are reported in Figure 4 and Table 3. Sample powders were collected from microbialites using a desktop-mounted drill press equipped with carbide drill bits ranging from 0.25 to 0.5 mm in diameter. Microdrilling targeted petrographically distinct phases in a succession from the core to the edge of several oncolites (Table 3). Additional measurements come from an incipient travertine crust encountered at the base of an alluvial fan that intersects the southeastern margin of the lake and two samples of marbles of early Paleozoic (?) age that crop out directly east of Laguna Negra.

Approximately 0.5 mg of microdrilled powder was loaded into silver capsules and processed via a Carbo-Flo automated sampling system. The Carbo-Flo system reacts sample powders with anhydrous phosphoric acid at 120 °C, cryogenically distills CO_2, and transports the resultant gas to a dual-inlet Finnigan MAT Delta Plus gas source IRMS. Carbon- and oxygen-isotope data are reported in delta notation as permil (‰) relative to the Vienna Pee Dee Belemnite (VPDB) standard. Analyses were reproducible to better than 0.1‰ for both $\delta^{13}C$ and $\delta^{18}O$, as determined by the analysis of replicate and internal laboratory standards. Two 50 mg samples obtained by microdrilling were bleached with hydrogen peroxide to eliminate organic matter, rinsed with pure water and analyzed for U/Th dating of carbonates.

Geochemical Modeling

Both aqueous speciation and mineral saturation indices were modeled using PHREEQC-I geochemical modeling software (Parkhurst and Appelo 1999; Charlton and Parkhurst 2002), using a hypothetical mixing of average lake and inlet waters. The input file for PHREEQC-I results is included in the online Supplementary Data file. Calculation of mineral Saturation Index (SI) is defined as the log IAP/K_{sp}; where IAP is the ionic activity product of calcium and carbonate ions, K_{sp} is the thermodynamic solubility constant for, in this case, calcite or aragonite, where SI = 0 is in equilibrium, < 0 is undersaturated, and > 0 is supersaturated.

LAKE WATER CHEMISTRY

The chemistry of Laguna Negra lake waters reflects the strongly negative water balance of the Puna region, and contrasts sharply with the composition

TABLE 3.—*Carbon and oxygen isotope data from Laguna Negra microbialites.*

Sample	$\delta^{13}C$ ‰ (VPDB)	$\delta^{18}O$ ‰ (VPDB)	Number of Analyses	Trendline (r^2)	Lamina type
MS1-A	8.87	0.31			Botryoidal to micritic
MS1-A′	8.29	−0.13			Botryoidal to micritic
MS1-B	8.49	−0.06			Botryoidal to micritic
MS1-C	8.75	−0.31			Botryoidal to micritic
MS1-D	8.86	0.35			Botryoidal to micritic
MS1-E	9.23	0.20			Botryoidal to micritic
MS1-F	10.75	1.80			Micritic
MS1-G	10.00	0.57			Micritic
MS1-I	10.15	1.11			Micritic
MS1-J	10.01	1.61			Micritic
			MS1 N=10	Y = 1.03X + 8.78 (r^2 = 0.82)	
MS2-A	10.86	0.27			Botryoidal to micritic
MS2-F	11.68	1.91			Botryoidal to micritic
MS2-G	12.65	1.29			Botryoidal to micritic
MS2-H	11.18	0.77			Botryoidal to micritic
MS2-I	10.03	0.14			Botryoidal to micritic
MS2-K	9.39	0.47			Botryoidal to micritic
MS2-M	9.31	0.59			Botryoidal to micritic
MS2-N	9.94	0.50			Botryoidal to micritic
MS2-O	10.21	−0.08			Botryoidal to micritic
MS2-P	11.16	0.77			Botryoidal to micritic
MS2-Q	9.24	−0.16			Botryoidal to micritic
MS2-R	9.86	0.81			Botryoidal to micritic
			MS2 N=12	Y = 1.25X + 9.70 (r^2 = 0.46)	
MS3-A	8.92	3.06			Peloidal cement
MS3-B	6.53	0.17			Isopachous
MS3-C	5.92	−0.49			Isopachous
MS3-D	6.10	0.05			Isopachous
MS3-F	6.39	−0.30			Isopachous
			MS3 N = 5	Y = 0.83X + 6.4 (r^2 = 0.97)	
MS4-A*	9.33	0.89			Isopachous
MS4-B	7.18	0.58			Isopachous
MS4-C	8.09	1.61			Micritic
MS4-D	7.74	1.23			Isopachous
			MS4 N = 3	Y = 0.88X + 6.7 (r^2 = 0.99)	
MS5-A	12.33	5.18			Isopachous to micritic
MS5-B	10.26	5.19			Isopachous to micritic
MS5-C	11.95	3.70			Isopachous to micritic
MS5-D	10.32	3.09			Isopachous to micritic
MS5-E	11.61	4.18			Isopachous to micritic
MS5-F	7.85	0.74			Isopachous to micritic
MS5-G	7.94	0.67			Isopachous to micritic
MS5-H	9.55	1.93			Isopachous to micritic
MS5-I	6.27	0.63			Isopachous to micritic
MS5-J	6.29	−0.25			Isopachous to micritic
			MS5 N = 10	Y = 1.01X + 6.9 (r^2 = 0.82)	
MS6-A	9.64	2.63			Isopachous to micritic
MS6-B	8.62	2.63			Isopachous to micritic
MS6-C	8.88	2.86			Isopachous to micritic
MS6-D	7.28	0.63			Isopachous to micritic
MS6-E	7.24	1.19			Isopachous to micritic
MS6-G*	4.31	0.01			Isopachous to micritic
			MS6 M = 5	Y = 0.94X + 6.5 (r^2 = 0.81)	
TRAV‡	14.69	0.04			Clotted Peloidal
CARB A‡	1.65	−11.58			Coarse sparry
CARB B‡	1.61	−13.17			Coarse sparry

Note: Alphabetic order indicates sampling for microdrilling from the core to the outside of oncoids and laminar crusts.
* Significant outlier not included in calculation of trendline
‡ Non-oncolitic carbonate, including a thin, groundwater seep travertine (TRAV.), and two Paleozoic marbles samples (CARB A and CARB B).

of inlet waters (Table 2). Lake water is a slightly acidic (average pH = 5.7), Ca-, Na-, and Cl-rich brine with an average salinity of 309‰, alkalinity of 833 mg/L, and [CO_2] of 3002 mg/L. By contrast, inlet waters, including surface runoff and groundwater seeps, are neutral to slightly alkaline (average pH of 7.7), with salinity of 18.5‰, alkalinity of 270 mg/liter, and CO_2 of 216 mg/liter. Average calcium, sodium, and chloride concentrations of inlet waters are substantially lower than lake waters. Sulfate concentrations can exceed that of lake waters by a factor of two. As expected, the composition of mixing zone waters is variable (cf. Table 2), reflecting the spatial heterogeneity of mixing and the differential influence of biology.

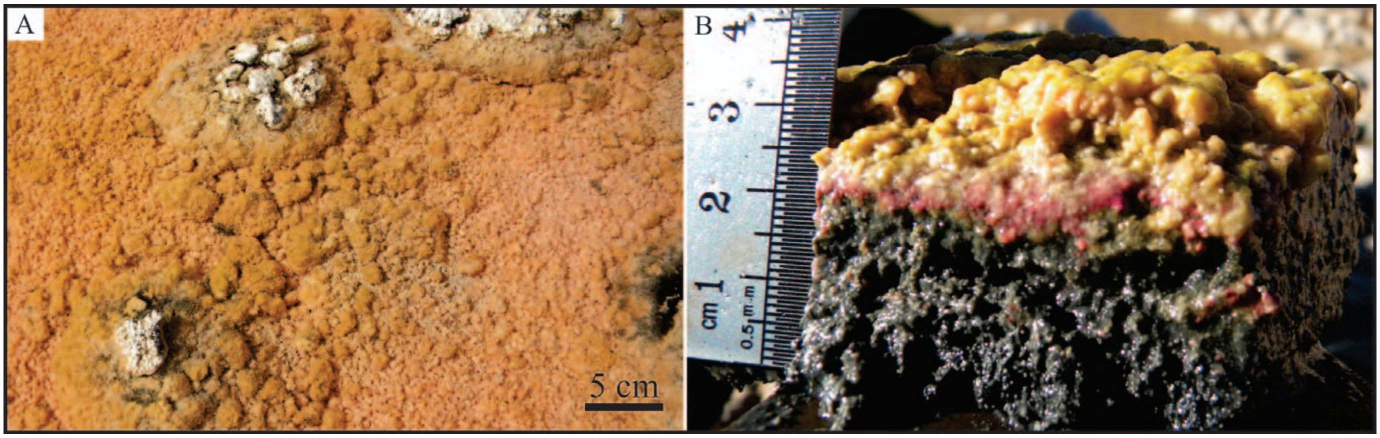

FIG. 5.—Typical Laguna Negra microbial mats. **A**) Orange-pink microbial mats and associated mineral precipitates that occasionally are partially exposed (light-colored mineral precipitates). **B**) Cross section of the microbial mats showing the stratified structure produced by different-colored lamina, with a diatom-cyanobacteria–rich upper layer, followed by purple and green sulfur bacteria in the undermat and underlain by a dark-colored horizon related to sulfate reduction and probably methanogenesis.

STABLE ISOTOPES OF MICROBIAL CARBONATES

The long-term environmental evolution of lake waters is, in part, reflected in the carbon- and oxygen-isotope composition of the microbialites and laminar crusts (Fig. 4; Table 3). Microbialites record O-isotope compositions that range from −0.49‰ to +5.19‰ and C-isotope compositions that range from +4.31‰ to +12.65‰, with individual microbialites displaying positive covariation between C- and O-isotopes ($r^2 > 0.82$ in most cases) that is characteristic of closed basin lakes (cf. Gasse et al. 1987; Talbot 1990). Isotopic values recorded in lake microbialites are also distinct from both travertine associated with local groundwater seeps ($\delta^{18}O$ = 0.04‰ and $\delta^{13}C$ = 14.69‰) and from lower Paleozoic marbles ($\delta^{18}O$ = −11.58 and −13.17, and $\delta^{13}C$ = +1.65 and +1.61, respectively) that may have interacted with local ground waters.

MICROBIAL MATS AND BIOFILMS

Environmental extremes (ultraviolet radiation influx, daily temperature variation, and elevated salinity) strongly limit the diversity of life in Laguna Negra. No fish occur in the lake; vascular plants are restricted to salt marsh species that occur only in proximal zones affected by fresh water influx; and copepods—although rare—have been observed in some proximal, low-salinity ponds. The standing biological community consists of a variety of mat-forming filamentous and coccoidal bacteria and colonies of centric, pennate, and filamentous diatoms. Microbial mats display a variety of stratiform, pustular, and pinnacle morphologies, and biofilms are common, coating the subaqueous carbonate and siliciclastic substrates. Mat structure, although variable, is similar to that observed in other hypersaline environments (Teske and Stahl 2002), with diatoms and photosynthetic cyanobacteria in the upper 1–5 mm of the mat, followed by anoxygenic purple- and green-sulfur bacteria in the undermat. These are, in turn, underlain by a thick black horizon with a distinct sulfurous odor that likely reflects bacterial sulfate reduction (Fig. 5). Preliminary 16SrRNA bacterial diversity analysis (Gomez et al., unpublished data) confirms the presence of representatives of these metabolic groups. The pervasive orange-pink to brown colors of surficial microbial mats (cf. Fig. 5) suggest elevated production of carotenoids and scytonemin-like pigments that may aid in protecting mat elements from high UV radiation influx and salinity stress (Gao and García-Pichel 2011).

MICROBIALITES AND LAMINAR CRUSTS

Microbialites and associated carbonate crusts of Laguna Negra are intimately associated with the microbial mat system and display a diverse set of morphologies, at both macroscopic (Fig. 6) and microscopic (Fig. 7) scale. Morphologies include mm- to cm-thick laminated crusts (Fig. 6A), which form patchy to laterally extensive pavements in the shallowest regions (Zones 3A and 3B) of Laguna Negra, and cm- to dm-scale concentrically laminated discs, spheres, and flattened domes that are herein referred to as oncoids (Fig. 6B–D). In addition to these discrete morphologies, oncoids also occur as complex composite structures (Fig. 6E, F). Oncoids are broadly distributed in Laguna Negra as both subaqueous and subaerially exposed surface accumulations (Zone 3C), and as discrete bodies within the upper meter of sediment.

Subaerially exposed oncoids constitute the bulk of the stromatolite belt and tend to be larger than subaqueous forms. Whether subaerial structures are permanently or seasonally exposed is unknown, because fluctuation in lake level has yet to be established. Growth of oncoids is represented by an accumulation of broadly concentric, smooth to irregular layers (Fig. 6G, H) defined by an alternation of colored laminae that range from white or dark-gray to green or red. Laminae appear to nucleate on a variety of substrates, including poorly lithified peloidal sediment, fragments of laminar crusts, or (more rarely) gravel-sized volcanic clasts. Many forms also show a series of external ridged protrusions (cf. Fig. 6C–D) occasionally overlapping at slightly different angles. In addition to lateral protrusions, many subaerially exposed oncolites also form mm-scale pillarlike protrusions, particularly located on the wind-affected side (cf. Fig. 6B).

The depositional age of these oncoids and associated mineral crusts is difficult to constrain. The scarcity of terrestrial organic matter and potentially large reservoir effects attributed to groundwater sources limit the utility of ^{14}C dating in these environments (cf. Valero-Garcés et al. 2000). Preliminary $U/Th_{carbonate}$ data from a partially buried oncoid from Laguna Negra yielded ages from 2442 ± 252 years at the core to 1057 ± 283 at the outer edge. In addition field observations and *in situ* carbonate precipitation experiments (data not shown) show that carbonate precipitation is, at present, actively occurring. Thus, these data suggest that carbonate deposition may have been active since ~ 2.4 ky and continues to the present.


A
B
C
D
E
F
G
H

MICROFABRIC OF MICROBIALITES

When observed petrographically, mineralized structures of Laguna Negra are composed of three primary lamina types: micritic, botryoidal, and isopachous (Fig. 7). Micritic (Fig. 7A–D) and botryoidal laminae (Fig. 7E–H) are variable in both thickness and degree of inheritance, and commonly produce changes in surface morphology. By contrast, isopachous laminae (Fig. 7I–L) show a high degree of inheritance and result in the translation and gradual smoothing of surface morphology. Additionally, hybrid laminae result from a combination of these end members. Differences in microfabric between laminated crusts, discs, and spheres are produced by changes in the proportion of these lamina types. In each case, lamina accretion is clearly controlled by mineral precipitation, with only rare trapping and binding of detrital sediment.

Micritic laminae occur as layers of irregular thickness (50–500 μm thick) composed of a complex heterogeneous mixture of micritic and microsparitic carbonate that retain a variety of smooth, peloidal, clotted, and tufted textures (Fig. 7A–D). Microbial filaments are locally preserved, and UV-fluorescence microscopy reveals an intimate association of micritic clots with organic matter. Microbial elements are most clearly observed as irregularly shaped clusters of red to orange coccoids. Under SEM (Fig. 8A), micritic laminae occasionally reveal a variety of hollow spheroids (up to 10 μm diameter) that represent putative microbial remains. The crystalline component of micritic laminae is composed of an array of nanometer-scale spherical, globular, or spherulitic calcite (typically less than 300 nm; Fig. 8B) or a dense mosaic of irregular globular to anhedral calcite crystals (cf. Fig. 8A). Similar aggregates have been observed within active biofilms (Fig. 8C–E) where nanoscale carbonate crystals precipitate within EPS matrices, preserving a variety of microbial and diatomaceous remains.

Micritic laminae are commonly associated with laminae containing individual or stacked botryoids (Fig. 7E–H). Botryoids consist of microlaminated (300 μm wide and 100 μm tall) or radial-fibrous (50–100-μm-wide and 400–600-μm-tall) crystal bundles that extend away from the substrate on which they nucleate. Individual botryoids are typically $<$ 500 μm thick and can stack to form laminae up to 4–5 mm thick. Petrographically, botryoids are commonly associated with clusters of pennate, centric, and filamentous diatoms and occasionally show evidence of associated bacterial components. UV-fluorescence intensity within botryoids shows rhythmic changes in intensity, revealing microlaminae with thicknesses generally $\leq$4 μm. Larger ($>$ 15 μm) spots of orange-to-red fluorescence mark incorporation of organic components associated with diatom frustules (Fig. 7H). Notably, nucleation points of individual botryoids show elevated fluorescence with respect to their external rims.

Isopachous laminae represent the third building block of the Laguna Negra microbialites (Fig. 7I–L). Isopachous laminae occur as encrustations over both micritic and botryoidal laminae, and are the principal component of laminated crusts. In addition, isopachous laminae can encrust peloidal sediments. Isopachous laminae consist of closely spaced, acicular calcite crystals comprising individual laminae 50–100 μm thick. Successive isopachous laminae are commonly separated by thin (10–50 μm) micritic horizons composed predominantly of irregularly shaped, anhedral to subhedral calcite crystals (Fig. 7L). Isopachous laminae are not associated with preserved microbial or algal elements, but frequently contain laterally persistent microlaminae ($<$ 5 μm) characterized by rhythmic changes in fluorescence.

DISCUSSION

Mixing Zone Model for Microbialite Mineralization

Several lines of evidence suggest that complex mixed-fluid interaction, strong evaporation and CO_2 degassing influenced the formation of Laguna Negra microbialites. Most critical is the position of the mineralized stromatolite belt at the interface between zones of freshwater influx and the main body of Laguna Negra. Secondly, O-isotope compositions for Laguna Negra microbialites (Fig. 4) are consistent with intense evaporation, yet are lower than that expected from Andean hypersaline lake waters (average $\delta^{18}O$ = +5‰ to +10‰; Risacher et al. 2003), suggesting precipitation from fluids variably influenced by isotopically light fresh water (average $\delta^{18}O = -10$‰; Risacher et al. 2003). Finally, although Laguna Negra receives most of its fluid input from snowmelt that interacts with andesitic-basaltic bedrock, its ionic composition contrasts with the theoretical ionic concentrations produced through evaporation of input waters. Elevated CO_2 concentration, as well as enrichment in Ca^{2+} and Cl^- of lake waters may reflect an additional input from a regional groundwater source that interacted with older carbonate- and evaporite-rich sedimentary rocks (cf. Risacher and Fritz 2009). Such multicomponent mixing has been proposed for the chemical evolution of similar lakes in Chile (Risacher and Fritz 2009; Lowenstein and Risacher 2009), although, in Laguna Negra, elevated CO_2 may reflect a combination of elevated CO_2 in regional groundwater (by interaction with either ancient carbonate rocks or volcanogenically influenced fluids) and localized microbial respiration of organic matter (cf. Duarte et al. 2008). Carbonate precipitation in Laguna Negra is restricted to the nearshore environments (where microbial mats are present), which is consistent with some influence of microbial activity.

C- and O-isotope compositions of the Laguna Negra microbialites (Fig. 4) are broadly comparable to values recorded in other Altiplano lacustrine carbonates (Valero-Garcés et al. 1999). O-isotope composition of these lacustrine carbonates appears to be influenced primarily by evaporation driven by the intense aridity of the Puna-Altiplano region, with elevated C-isotope values attributed to Rayleigh distillation associated with rapid degassing of high-CO_2 groundwater or extensive evaporation (Valero-Garcés et al. 2000). In closed basins, substantial variation in O-isotope composition may reflect the hydrologic balance of inflow waters and evaporation (Talbot 1990). Similarly, covariance of O- and C-isotope composition typically reflects degassing of CO_2 during evaporation, although changing productivity may also play a role (Talbot 1990; Jellison et al. 1996; Li and Ku 1997).

PHREEQC geochemical modeling (Parkhurst and Appelo 1999) was used to further explore the potential of fluid mixing on carbonate precipitation in Laguna Negra. Geochemical modeling of average lake water (Fig. 9) yields a calcite saturation index of 0.71, indicating oversaturation with respect to calcite. Although inlet waters are substantially more dilute than lake waters, their pH is relatively high, resulting in increased carbonate ion activity and a substantially greater saturation index of 1.21. Despite calcite oversaturation of lake and inlet waters, neither lake nor freshwaters actively precipitate abundant calcium carbonate. Rather, carbonate mineralization is restricted to a shallow-water margin that marks the mixing zone between hypersaline lake waters and more dilute fresh waters (Fig. 10). The mixing zone of chemically unlike fluids can result in complex (nonlinear) chemical behavior where both precipitation and dissolution can occur, based on experimental and

←

FIG. 6.—Laminar crusts and Oncoids morphologies typical of Zones 3A and 3C. **A**) Laminar crusts. **B**) Discoidal structure. **C**, **D**) Subspherical structures, note the presence of partially rotated structures in C). **E**, **F**) Composite structures. **G**, **H**) Polished cross sections showing the complex internal concentric lamination and changes in color during lamina accretion probably related to trace element and organic matter incorporation during carbonate precipitation. Note the presence of irregular surface ornamentations of calcite (B), mostly located on the side affected by winds (red arrow). The longest axes are 35 cm, 30 cm, 20 cm, 25 cm, 60 cm in Parts B, C, D, E, and F respectively; 10 cm in G, and 8 cm in H.

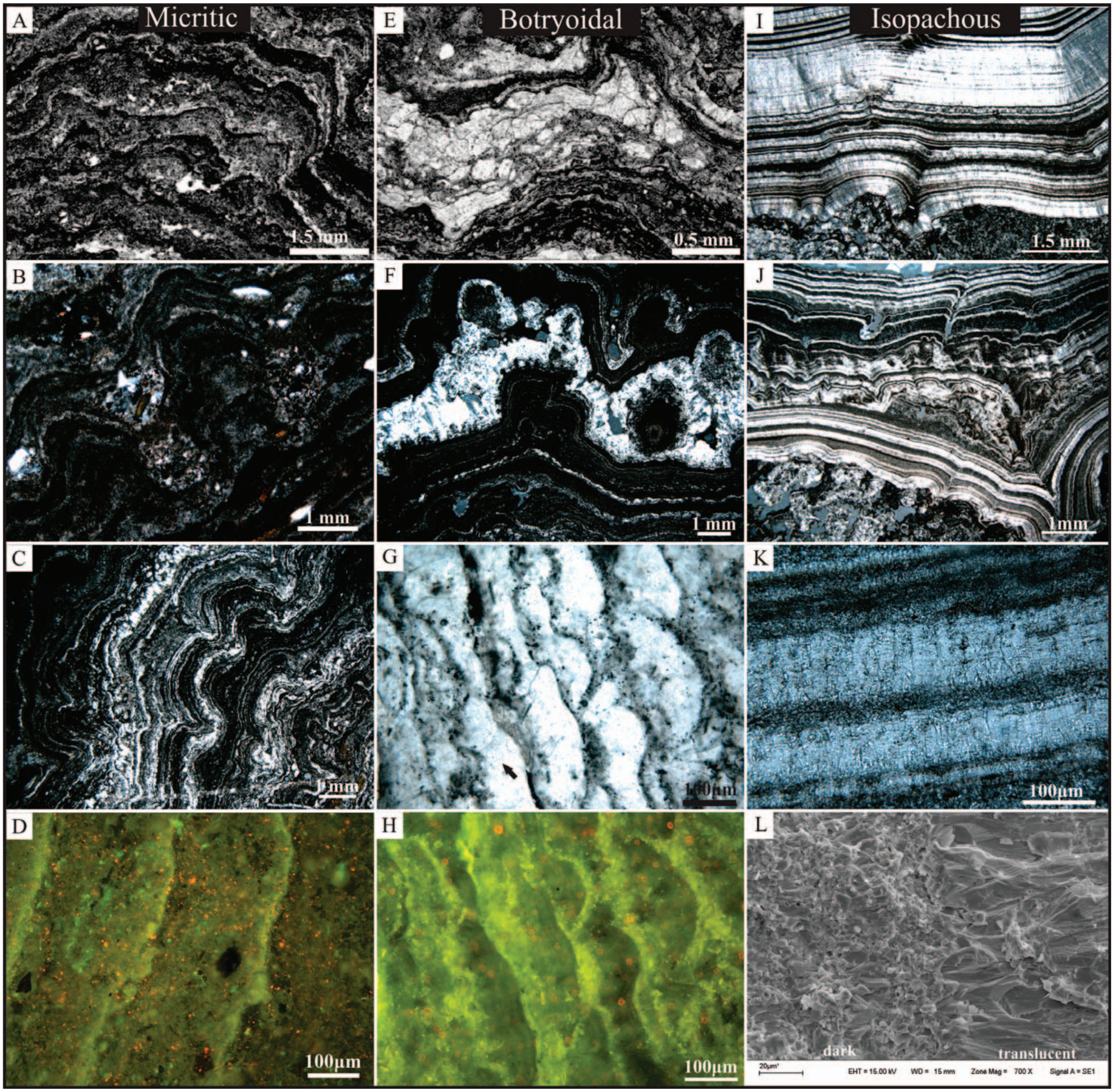

FIG. 7.—Microscopic textures of the three main types of laminar components: irregular micritic, botryoidal, and isopachous. **A–D**) Irregular micritic to microsparitic laminae occasionally alternating with irregular botryoidal laminae (translucent laminae in E–H), which usually are intimately associated. **D**) Under UV light, micritic laminae show strong fluorescence due to organic-material incorporation during lamina accretion. **E–H**) Irregular lamina preferentially formed by stacked botryoidal crystals that usually alternate with irregular micritic laminae. **G**) Dark-colored areas of degraded organic remains and diatom frustules between stacked crystals. **H**) A UV-fluorescence image showing the fluorescence due to incorporation of organic material during precipitation (see text for details). **I–K**) Petrographic microscope images of isopachous laminae produced by regular alternation of bright (sparry) and dark (micritic) laminae. **L**) SEM image showing that sparry lamina are mostly represented by microlaminated, elongated, radial crystals and dark-colored laminae are represented by equidimensional, irregularly shaped, subhedral to anhedral crystals less than 5 µm in diameter.

geological examples (Berkowitz et al. 2003; Singurindy et al. 2004). In Laguna Negra, regions of carbonate mineralization have higher pH (to 6.9–7.2) than average lake waters, indicating mixing with local inlet waters. Increased carbonate ion activity associated with elevated pH is marked in our geochemical modeling as an increase in calcite saturation index (SI = 1.37; an increase of nearly 93% over average lake waters) that occurs with mixing of lake and inlet waters at ratios between 1:1 and 1:3. Since the zone of mineralization corresponds spatially to this mixing zone (Fig. 10), we suggest that substantial calcite oversaturation is critical to the initiation of carbonate precipitation. We consider that the increase in

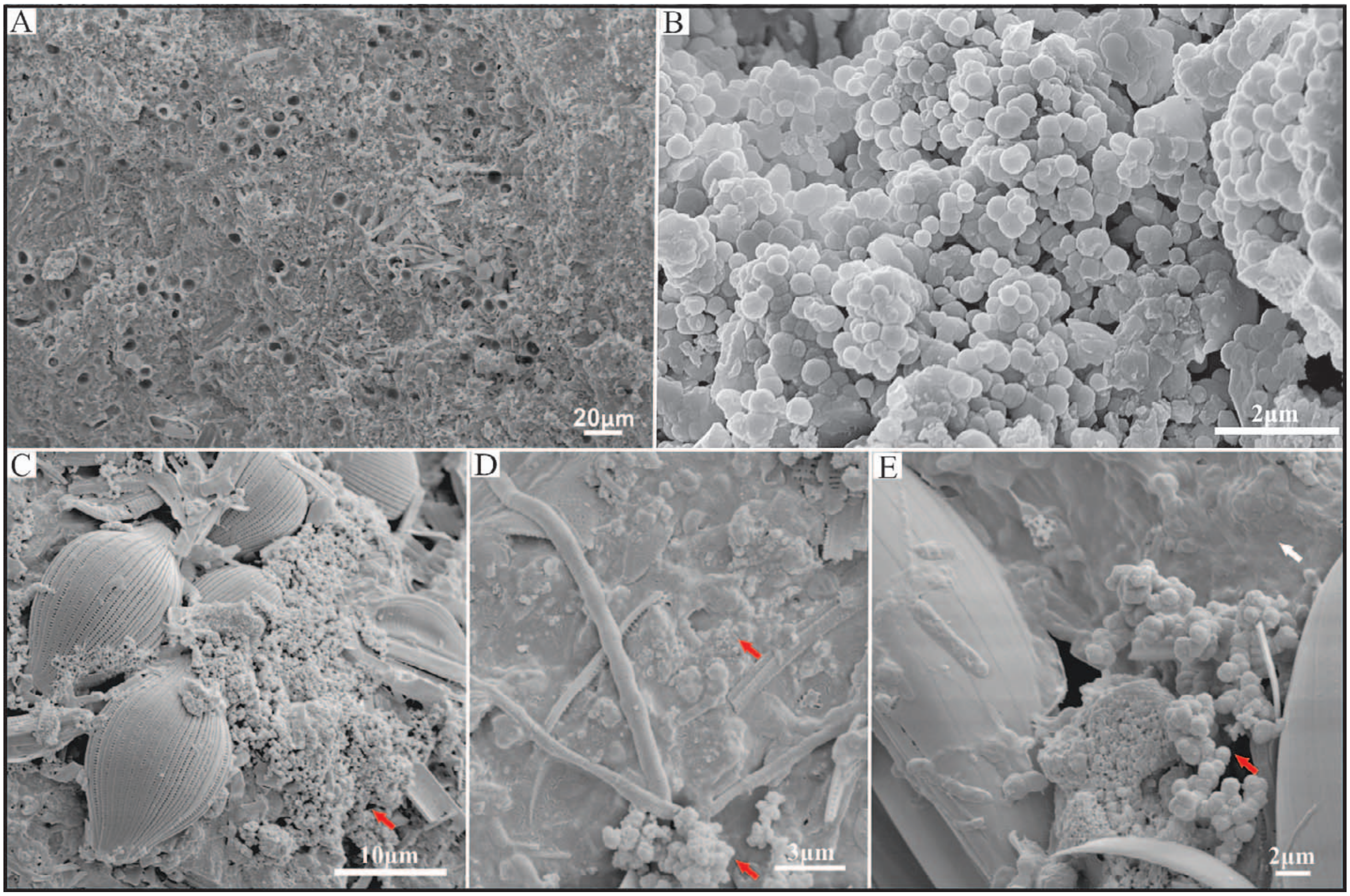

FIG. 8.—**A**, **B**) SEM images of irregular micritic laminae in the Oncoids. Note the presence of subspherical to globular nanoaggregates as the main component of these micritic laminae. Spherical voids likely represent organic matter that was entombed and later degraded. **C**–**E**) These nanoaggregates are also observed in currently active biofilms, where these nanoparticles preferentially occur inside an EPS matrix (red arrow shows exposed nanoaggregates and white arrow indicates nanoaggregates within the EPS matrix) in diatom-cyanobacteria–rich biofilms, suggesting a similar origin for those aggregates recorded in the structures.

calcite saturation in the mixing zone, combined with microbial mat activity, which can affect local carbonate equilibrium either actively (via metabolic activity that enhances local CO_2 concentrations) or passively (via production of sites for carbonate mineral nucleation), are both critical to the development of the Laguna Negra stromatolite belt. We also suggest that, in addition to the mixing related increase in carbonate saturation, the contribution of dilute waters may be sufficient to reduce salt stress or to provide additional necessary nutrients for development of an extensive microbial community (cf. Krammer et al. 2008).

Furthermore, although CO_2 degassing during intense evaporation likely provides the initial pool of isotopically enriched carbon, we suggest that elevated C-isotope compositions of Laguna Negra microbialites may also reflect influence of photosynthetic drawdown of CO_2 and/or microbial methanogenesis (cf. Talbot and Kelts 1990), which can be important in controlling C-isotope signature in sulfate-poor lakes such as Laguna Negra. The botryoidal and micritic laminae of Laguna Negra, which both reflect biologically influenced precipitation, record C-isotope values (7.0‰–13.0‰, Table 3) substantially higher than regional lake waters (Valero-Garcés et al. 2000). In this case, locally enhanced microbial activity may result in net CO_2 drawdown and ^{13}C enrichment, despite petrographic evidence that microbial decomposition plays a role in mineral nucleation. A more detailed isotopic study is currently underway to unravel environmental and biological controls on the C-isotope composition of Laguna Negra microbialites.

Morphology of the Laguna Negra Microbialites

The bulk of the stromatolite belt is represented by concentrically laminated spherical to discoidal structures where lamina accretion occurs by a combination of environmental and biological processes. Lateral ridged protrusions appear to correspond to preferential growth at the water line and/or sediment-water interface, potentially via salt accumulation at the oncolite surface. Macro-scale protrusions and internal lamination overlapping at different angles clearly demonstrate at least episodic rotation of oncoids. Although movement of at least some oncoids could result from local winds exceeding the threshold shear velocity for movement (cf. Milana 2009, who records winds as high as 443.2 km/hr in the Puna region), rotation of partially exposed, large (> 30 cm) oncoids more likely results from lateral pressure changes and displacement of oncoids associated with either salt or ice formation. In winter, where dilute waters at the lake edge freeze, substantial deformation of the substrate has been observed. Alternatively, rotation may result from localized medium fluidization during episodic seismic events, although this has not been recorded.

Although episodic rotation of oncoids has occasionally occurred, the concentric nature of lamination is best explained by *in situ* growth by diffusion of calcium and bicarbonate ions at similar rates around the structures, with accretion on the underside occurring by displacive crystal growth inside an organic matrix (cf. Risacher and Eugster 1979; Hägele

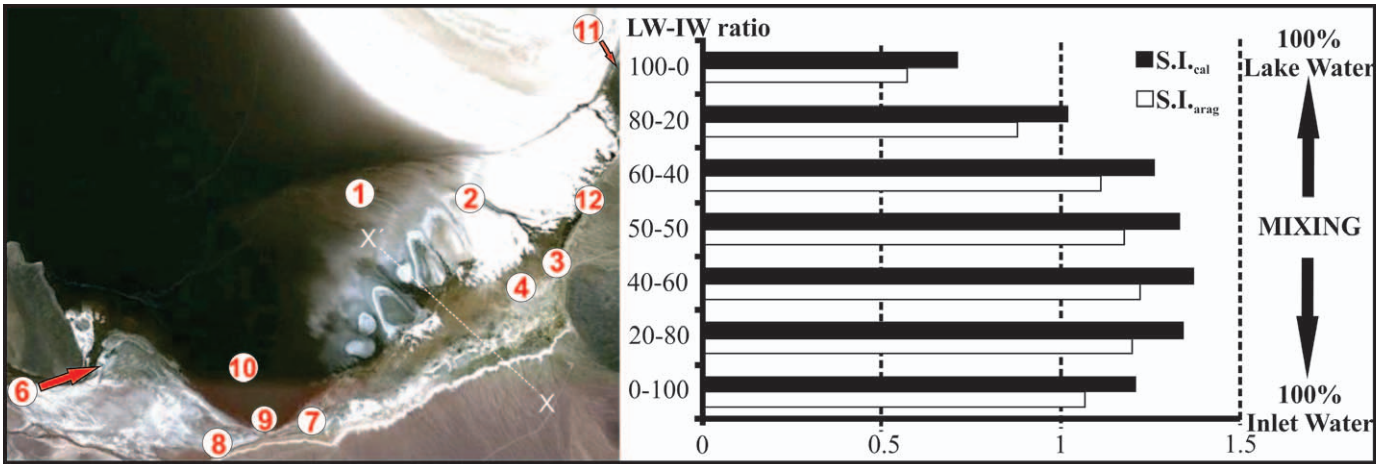

FIG. 9.—**A**) Sampling points for water chemistry (see also Table 2). **B**) Output of geochemical modeling with PHREEQC showing how the saturation index for calcite and aragonite (SI_{cal} and SI_{arag}, respectively) changes under different mixing ratios of average lake (LW) and inlet (IW) waters.

et al. 2006). Additionally, development of discoidal shapes likely reflects preferential precipitation along either the air-water or sediment-water interface.

The generally concentric nature of most mineralized structures suggests formation when submerged, but it is clear that at least some irregular lamina accretion can occur even during subaerial exposure. Salt encrustations, including lateral ridges at the air-water interface, mm- to cm-scale pillars and preferentially thicker laminar crusts on the windward side of exposed microbialites are often incorporated into the overall lamina structure of oncoids. In these cases we suggest that lamina accretion results, in part, from moisture from wind, spray, or wind-induced waves followed by precipitation triggered by rapid evaporation and degassing. Similar processes also have been recorded by several authors in the genesis of stromatolites and mineral crusts, for example in aragonite splash crusts in modern tidal flats (Trucial Coast, Persian Gulf, Purser and Loreau 1973; Alsharhan and Kendall 2003), in siliceous sinters (cf. Handley et al. 2005, 2008), and laboratory experiments (McLoughlin et al. 2008).

Genesis of Microbial Microfabrics—Micritic Laminae

Irregular, wrinkled, peloidal, and clotted textures in micritic and botryoidal lamina, as well as both abundant organic remains and apparent incorporation of dissolved organic carbon, suggest mineral precipitation associated with microbial biofilm activity. Irregular, peloidal, and clotted micritic textures have been recorded for microbial carbonates elsewhere (Riding 2000, 2008; Pedley 2000; Riding and Awramik 2000), and other studies have also noted organic matter incorporation during carbonate precipitation (cf. Guido et al. 2012). Although several inorganic ions can produce fluorescence, cathodoluminescence reveals only dull luminescence (related to low concentrations of Mn^{2+}, which is a primary activator, Shopov 2004). Additionally, observed variation in UV fluorescence is at a scale much finer than that observed under cathodoluminescence, suggesting that the main control on fluorescence is organic matter incorporated into the carbonates, rather than variation in carbonate trace element content.

Well-developed biofilms provide active nucleation sites for carbonate mineralization, can affect local calcium carbonate equilibrium due to metabolic activity (Riding 2000; Dupraz et al. 2009; Arp et al. 2012), and can control diffusion of calcium and carbonate ions (Stewart 2003; Bissett et al. 2008), thereby influencing carbonate precipitation (and/or inhibition of precipitation; Heath et al. 1995; Kawaguchi and Decho 2002) and microfabric development (Bosak and Newman 2003; Braissant et al. 2003; Chekroun et al. 2004). Decomposition of microbial elements, in particular EPS, can result in preferential release of Ca^{2+}, thereby increasing the efficacy of carbonate mineral nucleation (Visscher and Stolz 2005; Decho 2010). SEM images of Laguna Negra microbialites (Fig. 8) commonly show nanometer-size globular, botryoidal, and spherulitic particles and aggregates which occur within the EPS matrix of active biofilms (see also Vasconcelos et al. 1995; Defárgue et al. 1996; Bosak and Newman 2003; Visscher and Stolz 2005; Aloisi et al. 2006; Bontognali et al. 2008; Defárgue 2010; Decho 2010; Perri et al. 2012; Manzo et al. 2012; Jones and Peng 2012). That mineral precipitation tends to entomb cyanobacterial sheaths,

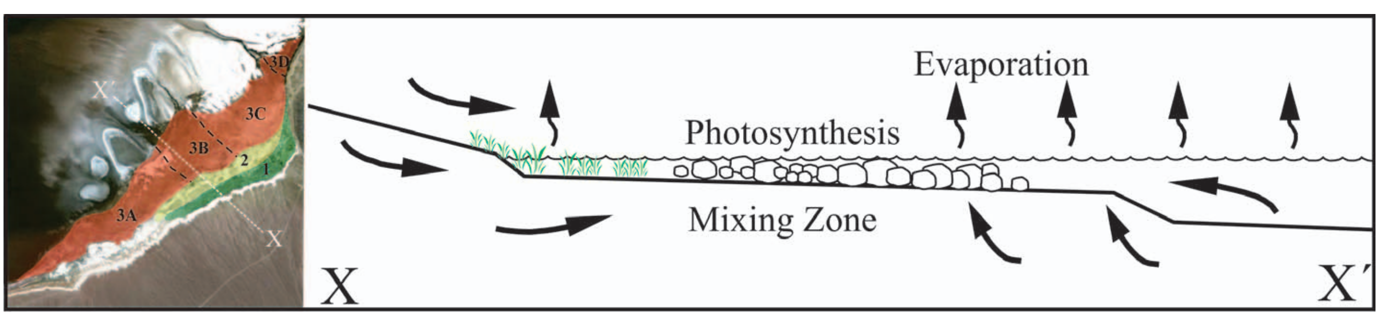

FIG. 10.—Schematic cross-section view (X–X′) of the mixing zone. Water depth in the ponds located in the mixing zones is up to 10–15 cm. In this model, regional evaporation, mixing of lake waters with inlet waters, and microbial activity maximize carbonate saturation and trigger mineralization of microbial components (see text for details).

coccoids, and diatom frustules rather than nucleate on the organic remains of these organisms, suggests that mineralization was mostly related to degradation of the EPS matrix (Trichet and Defárgue 1995; Defárgue 2010).

Although calcite represents the dominant phase of calcium carbonate, nanophase spherules observed under SEM could have precipitated as amorphous calcium carbonate (ACC) (cf. Jones and Peng 2012). ACC can be stabilized by the presence of organic material (Bentov et al. 2010; Jones and Peng 2012) as well as inorganic ions like Mg^{2+} (Politi et al. 2010), although it generally transforms rapidly into crystalline calcite (Ajikumar et al. 2005; Goodwin et al. 2010; Rodriguez-Blanco et al. 2011; Jones and Peng 2012). Further study is needed to test this mechanism in Laguna Negra, since verification of ACC has not been possible under XRD, mostly because the presence of crystalline phases like calcite and aragonite make the detection of amorphous phases more difficult (cf. Jones and Peng 2012).

Genesis of Microbial Microfabrics—Botryoidal (Sparry) Laminae

Irregular sparry laminae, represented by individual and stacked botryoidal crystals, are intimately associated with micritic laminae. As with micritic laminae, botryoidal elements are associated with organic remains and incipient biofilms. Notably, organic material appears to provide primary nucleation sites for botryoidal crystals, which then grow and entomb the organic material. This relationship suggests that organic decomposition reactions triggered carbonate precipitation by increasing alkalinity and ionic activity, or by providing suitable sites for mineral nucleation. Microbes and diatoms were then passively entombed and preserved during later fast crystal growth. Because diatoms typically produce high amounts of exopolymeric substances (EPS) as protection against both water and salinity stress (Wotton 2004), we suggest that botryoidal laminae may represent nucleation and passive growth of carbonate crystals on EPS accumulations. Microlamination observed under luminescence further suggests short-term changes in saturation state and crystal growth rate, potentially controlled by fluctuations in temperature or salinity.

Similar sparry textures have been recorded where botryoidal aggregates and crystal fans develop in protected environments of cyanobacteria and diatomaceous EPS (Monty and Hardie 1976; Winsborough and Golubic 1987; Winsborough et al. 1994; Winsborough 2000; Arp et al. 1999). We suggest that both sparry and micritic lamination can be produced by seasonally induced environmental changes (cf. temperature, water chemistry, nutrient influx) that affect biofilm development, mineral supersaturation, mineral nucleation, and subsequent crystal growth. In this scenario, nucleation of botryoids and development of sparry laminae may be triggered by decomposition of biofilms. Once crystal nucleation is triggered, crystal growth occurs and entombs associated organic material. By contrast, micritic laminae occur when local biofilms are better developed and exert a stronger control on microfabric development. Seasonal controls for the development of sparry and micritic textures have been recorded for modern tufas (Perri et al. 2012; Arp et al. 2001). Sampling during the summer of 2011 showed preferential development of micrite textures inside EPS-rich diatom biofilms which is consistent with this scenario, although sampling has not yet been possible to evaluate seasonal changes in biofilm and microbial mat structure.

Genesis of Microbial Microfabrics—Isopachous Lamina

In contrast to irregular micritic and botryoidal fabrics, isopachous laminae do not show a strong association with biofilm that could control microtextures by modifying ion diffusion (Stewart 2003) and controlling crystal nucleation and growth (Bissett et al. 2008). This explains the lamina regularity and high degree of inheritance during lamina accretion and suggests that this fabric is dominantly produced by abiotic precipitation of carbonate. Isopachous laminae are most prevalent in laminar crusts that form in the shallowest portions of Laguna Negra (Zone 3A, better connected with the main lake, Fig. 3). Isopachous laminae also form on subaerially exposed surfaces of oncoids, where spray effects and rapid evaporation produce a combination of smooth to irregular (microdigitate) structures of abiotic origin. The presence of microlamination further suggests, as with botryoidal phases, short-term changes in saturation state and crystal growth rate that are potentially controlled by fluctuations in temperature or salinity.

IMPLICATIONS

Laguna Negra Microbialites as a Precambrian Analogue

Although the macroscopic morphology of microbialites in Laguna Negra differs substantially from Proterozoic forms, preserved laminated microfabrics are strikingly similar to those found across a range of well-preserved Proterozoic stromatolites (Fig. 11) (Kah and Knoll 1996; Knoll and Semikhatov 1998; Pope and Grotzinger 2000; Bartley et al. 2000; Seong Joo and Golubic 2000; Pope et al. 2000; Riding 2008; Knoll et al. 2013). Furthermore, certain elements of geochemistry and ecology within Laguna Negra are plausibly similar to a variety of Proterozoic nearshore environments, suggesting parallels in the mechanisms of precipitation and lamina accretion. Chemically controlled precipitates in the geologic record are typically represented by regular isopachous laminites and botryoidal crusts composed of radial fibrous crystals (cf. Kah and Knoll 1996; Bartley et al. 2000; Seong Joo and Golubic 2000; Kah et al. 2001, 2006, 2012; Knoll et al. 2013; collectively called sparry crusts, cf. Riding 2008). The remarkable uniformity in thickness, lateral continuity, high degree of inheritance during lamina accretion, and development of microdigitate structures have been interpreted to record precipitation at the sediment-water interface from oversaturated waters, in which biological participation is insignificant or absent (Pope and Grotzinger 2000; Knoll and Semikhatov 1998; Bartley et al. 2000; Pope et al. 2000). Microfabrics that show a greater influence of microbial activity are typically represented by irregular, wrinkled, peloidal micritic crusts, micritic clots, clumps, and veneers, and hybrid crusts (Riding 2008). Here nucleation of small (micrite-size) crystals predominates over development of large crystals. Microlaminated botryoidal crystals nucleated on degraded organics, including organics during later crystal growth, as recorded in Laguna Negra, have also been recorded in the Precambrian (Knoll and Semikhatov 1998; Bartley et al. 2000). The growth mechanism described here could help explain why excellent microfossil preservation is often associated with this fabric (Bartley et al. 2000).

Laguna Negra oncoids show the same basic building blocks as Precambrian microbialites (Riding 2008), and likely developed under remarkably similar geochemical conditions. Mineral precipitation occurs by a combination of subaqueous and subaerial process with different degrees of biological participation, resulting in a wide spectrum of microfabrics. In Laguna Negra, increased carbonate saturation, driven by a combination of sustained evaporation and episodic fluid mixing, appears to play a principal role in the spatial distribution of carbonate precipitation. Similar processes of fluid mixing and evaporation could have played a role in lamina accretion in peritidal subaerial environments in the Precambrian, and we suggest that such processes need to be considered when studying the record of ancient microbial deposits from ancient tidal flats (or marginal lacustrine zones). Similar micritic, botryoidal, and isopachous laminae in Proterozoic strata (cf. Atar Group, Bertrand-Sarfati 1976; Kah et al. 2012; Society Cliffs Formation, Kah and Knoll 1996; Gaoyuzhuang Formation, Seong-Joo and Golubic 1999; Billyakh Group, Bartley et al. 2000) occur in nearshore environments, which plausibly experienced both elevated carbonate saturation and episodic freshwater influx. Unlike Laguna Negra, the primary mechanism for elevated carbonate saturation in the Proterozoic was globally high pCO_2 (Grotzinger and Kasting 1993; Bartley and Kah

FIG. 11.—Three examples of comparable microtextures typically recorded in Precambrian microbial carbonates: **A**) Irregularly laminated micritic to microsparitic microtextures commonly recorded within flat-laminated, peritidal microbial facies (~ 1.1 Ga Society Cliffs Formation, Bylot Supergroup, northern Baffin Island, Canada). Brown-colored micrite (red arrow) is associated with organic-rich laminae (and when preserved in early diagenetic chert, associated with partially degraded thick-filamentous mats—see Knoll et al. 2013). Microspar is associated with alternating laminae composed of tightly woven, thin filament mats (cf. Knoll et al. 2013). Larger, nodular regions containing gray micrite (black arrow) correlate, when preserved in chert, to thick accumulations of EPS, often associated with coccoidal mat communities. **B**) Microlaminated precipitates, interlaminated with microbial breccia, and containing large botryoids (black arrow) preserved in early diagenetic chert (1.27 Ga Greenhorn Formation in the Dismal Lakes Group, Arctic Canada). **C**) Flat-laminated microbial carbonates largely represented by isopachous cement laminae, now replaced by fabric-retentive dolomite (1.27 Ga Greenhorn Formation in the Dismal Lakes Group, Arctic Canada).

2004), with regional modification by evaporation (cf. Kah et al. 2001, 2012) and photosynthetic drawdown (Knoll et al. 2013). Freshwater influx in at least some units has been inferred by the presence of the microfossil *Archaeoellipsoides* (Sergeev et al. 1995), which has been interpreted as a heterocystous cyanobacterial akinete associated with brackish-water environments (Golubic et al. 1995). Combined, similarities between Laguna Negra microbialites and Proterozoic stromatolite fabrics suggest that zones of fluid mixing may have been similarly important in comparably ancient settings.

Astrobiology Implications

Geochemical modeling of acidic environments on Mars suggests poor preservation potential for organic matter (Sumner 2004) and water activity below the threshold to sustain life (Tosca et al. 2008). Mixing zones in evaporitic systems on early Earth or Mars could therefore be a potential exploration target by providing a habitable environment by local increase of water activity (and nutrient availability), and by triggering precipitation reactions favorable to the preservation of organic remains (cf. Zavarzin et al. 2003). The recent record of martian minerals related to aqueous geochemistry (Murchie et al. 2009), particularly carbonate deposits (Morris et al. 2010), and evaporative playa-lake systems (Di Achille et al. 2009; Andrews-Hanna et al. 2010), further highlights the astrobiological potential to understand microbial life in hypersaline lakes and their potential biosignatures. The potential for mixing zones as favorable taphonomic windows has already fostered investigations, for example, in settings like Shalbatana Vallis (Di Achille et al 2009) where lacustrine strandlines and putative fan-delta deposits have been identified (Di Achille et al. 2009; Komatsu et al. 2009).

We consider that the mineralizing microbial system in Laguna Negra is a unique natural laboratory that fulfills the environmental criteria suggested for early Earth and Mars and where a spectrum of ongoing biotic and abiotic process and potential biosignatures can be studied and tested, improving our ability to interpret the sedimentary record on our planet and beyond.

CONCLUSIONS

In the Laguna Negra microbialites we recognize complex layering produced by the interplay of carbonate fabric types: microbially associated micrite, botryoidal precipitates, and isopachous cement phases. These represent a continuum of biological influence on carbonate nucleation and growth within a carbonate-oversaturated mixing zone. Laguna Negra microbialite microtextures are remarkably similar to Precambrian analogues, suggesting similar controls on microfabric development influenced both modern and ancient microbialites. Geochemical modeling suggests that mixing between groundwater and lake water, together with evaporation and CO_2 degassing, play a central role in controlling carbonate saturation and the loci of carbonate precipitation. Stable isotope analyses indicate significant CO_2 degassing during evaporation, as typically found in closed-lake systems. Although evaporation and degassing likely provide an initial pool of isotopically heavy carbon, we suggest that further modification of C-isotope compositions occurred due to biological influences such as photosynthetic drawdown of CO_2 and/or microbial methanogenesis. These results underscore the importance of hydrological mixing zones in controlling the development of microbialite-bearing facies and the role of these facies as taphonomic windows that may preserve evidence of microbial activity in both terrestrial and martian settings.

ACKNOWLEDGMENTS

Funding was provided by the NASA Planetary Biology Internship program, SARIF (Scholarly Activity and Research Incentive Funds) and Professional Development awards from the University of Tennessee. Also by the Agencia Nacional de Promoción de Ciencia y Técnica (ANPCyT), projects PICT 1306, 33630, Consejo Nacional de Investigaciones Científicas y Técnicas (CONICET) and Secretaria de Ciencia y Técnica, Universidad Nacional de Córdoba (SECYT-UNC) project 214/10-11, and the CICTERRA (Centro de Investigaciones en Ciencias de la Tierra). We thank G. Gilleaudeau, C. Thompson, Jose María Tello, Luciano Montoya, and M. Argota for field assistance; and Z. Li for assistance in isotopic analysis. We also appreciate comments from the Associate Editor (Stephen T. Hasiotis) and the reviewers Robert Riding and Frank Corsetti that significantly strengthened our interpretations to the benefit of our work.

SUPPLEMENTAL MATERIAL

Data is available from the PALAIOS Data Archive: http://www.sepm.org/pages.aspx?pageid=332.

REFERENCES

Ajikumar, P.K., Wong, L.G., Subramanyam, G., Lakshminarayan, R., and Valiyaveettil, S., 2005, Synthesis and characterization of monodispersed spheres of amorphous calcium carbonate and calcite spherules: Crystal Growth and Design, v. 5, p. 1129–1134.

Allwood, A.C., Walter, M.R., Kamber, B.S., and Burch, I.W., 2006, Stromatolite reef from the early Archaean era of Australia: Nature, v. 414, p. 714–718.

Aloisi, G., Gloter, A., Wallmann, K., Guyot, F., and Zuddas, P., 2006, Nucleation of calcium carbonates on bacterial nanoglobules: Geology, v. 34, p. 1017–1020.

Alsharhan, A.S., and Kendall, C.G.St.C, 2003, Holocene Coastal carbonates and evaporites of the southern Arabian Gulf and their ancient analogues: Earth-Science Reviews, v. 61, p. 191–243.

Andrews-Hanna, J.C., Zuber, M.T. Arvidson, R.E. and Wiseman, S.M., 2010, Early Mars hydrology: Meridiani playa deposits and the sedimentary record of Arabia Terra: Journal of Geophysical Research, v. 115, E06002, doi: 10.1029/2009 JE003485.15.

Arp, G., Helms, A., Karlinska, K., Schumann, G., Reimer, A., Reitner, J., and Trichet, J., 2012, Photosynthesis versus Exopolymer Degradation in the Formation of Microbialites on the Atoll of Kiritimati, Republic of Kiribati, Central Pacific Geomicrobiology Journal, v. 29, p. 29–65.

Arp, G., Thiel, V., Reimer, A., Michaelis, W., and Reitner, J., 1999, Biofilm exopolymers control microbialite formation at thermal springs discharging into alkaline Pyramid Lake, Nevada, USA: Sedimentary Geology, v. 126, p. 159–176.

Arp, G., Reimer, A., and Reitner, J., 2001, Fluvial tufa formation in hard-water creek (Deinschwanger Bach, Franconian Alb, Germany): Facies, v. 44, p. 1–22.

Awramik, S.M., and Buchheim, H.P., 2009, A giant, late Archean lake system: the Meentheena Member (Tumbiana Formation; Fortescue Group), Western Australia: Precambrian Research, v. 174, p. 215–240.

Bartley, J.K., and Kah, L.C., 2004, Marine carbon reservoir, C_{org}–C_{carb} coupling, and the evolution of the Proterozoic carbon cycle: Geology, v. 32, p. 129–132.

Bartley, J.K., Knoll, A.H., Grotzinger, J.P., and Sergeev, V.N., 2000, Lithification and fabric genesis in precipitated stromatolites and associated peritidal carbonates, Mesoproterozoic Billyakh Group, Siberia, *in* Grotzinger, J.P., and James, N.P., eds., Carbonate Sedimentation and Diagenesis in the Evolving Precambrian World: Society for Sedimentary Geology (SEPM) Special Publication 67, p. 59–63.

Bentov, S., Weil, S., Glazer, L., Sagi, A., and Berman, A., 2010, Stabilization of amorphous calcium carbonate by phosphate rich organic matrix proteins and by single phosphoamino acids: Journal of Structural Biology, v. 171, p. 207–215.

Berkowitz, B., Singurindy, O., and Lowell, R.P., 2003, Mixing-driven diagenesis and mineral deposition: $CaCO_3$ precipitation in salt water–fresh water mixing zones: Geophysical Research Letters, v. 30, issue 5, 1253, doi: 10.1029/2002GL 016208.

Bertrand-Sarfati, J., 1976, An attempt to classify late Precambrian stromatolite microstructures, *in* Walter, M.R., ed., Stromatolites: Developments in Sedimentology, vol. 20: Amsterdam, Elsevier, p. 251–259.

Bissett, A., Reimer, A., De Beer, D., Shiraishi, F., and Arp, G., 2008, Metabolic microenvironmental control by photosynthetic biofilms under changing macroenvironmental temperature and pH conditions: Applied and Environmental Microbiology, v. 74, p. 6306–6312.

Bontognali, T.R.R., Vasconcelos, C., Warthmann, R.J., Dupraz, C., Bernasconi, S.M., and Mckenzie, J.A., 2008, Microbes produces nanobacteria-like structures, avoiding cell entombment: Geology, v. 36, p. 663–666.

Bosak, T., and Newman, D.K., 2003, Microbial nucleation of calcium carbonate in the Precambrian: Geology, v. 31, p. 577–580.

Boschetti, T., Cortecci, G., Barbieri, M., and Mussi, M., 2007, New and past geochemical data on fresh to brine waters of the Salar de Atacama and Andean Altiplano, northern Chile: Geofluids, v. 7, p. 33–50.

Braissant, O., Cailleau, G., Dupraz, C., and Verrecchia, E.P., 2003, Bacterially induced mineralization of calcium carbonate in terrestrial environments: the role of exopolysaccharides and amino acids: Journal of Sedimentary Research, v. 73, p. 485–490.

Buick, R., 1992, The antiquity of oxygenic photosynthesis: evidence from stromatolites in sulphate-deficient Archaean lakes: Science, v. 255, p. 74–77.

Burne, R.V., and Moore, L.S., 1987, Microbialites: organosedimentary deposits of benthic microbial communities: PALAIOS, v. 2, p. 241–254.

Charlton, S.R., and Parkhurst, D.L., 2002, PHREEQC-I: A graphical user interface to the geochemical model PHREEQC: U.S. Geological Survey Fact Sheet FS-031-02, 2 p. http://wwwbrr.cr.usgs.gov/projects/GWC_coupled/phreeqci/.

Chekroun, K.B., Rodriguez-Navarro, C., Gonzalez-Munoz, M.T., Arias, J.M., Cultrone, J., and Rodriguez-Gallego, M., 2004, Precipitation and growth of calcium carbonate induced by *Myxococcus xanthus*: implications for recognition of bacterial carbonates: Journal of Sedimentary Research, v. 74, p. 868–876.

Cuerno, R., Escudero C, García-Ruiz, J.M., and Herrero, M.A., 2012, Pattern formation in stromatolites: insights from mathematical modeling: Journal of the Royal Society Interface, v. 9, p. 1051–1062.

Decho, A., 2010, Overview of biopolymer-induced mineralization: What goes on in biofilms?: Ecological Engineering, v. 36, p. 137–144.

Defárgue, C., 2010, Organomineralization, *in* Reitner, J., and Volker, T., eds., Encyclopedia of Geobiology: Springer, Dordrecht, The Netherlands, p. 697–701.

Defárgue, C., Trichet, J., Jaunet, A.M., Robert, M., Tribble, J., and Sansone, F.J., 1996, Texture of microbial sediments as revealed by cryo-scanning electron microscopy: Journal of Sedimentary Research, v. 66, p. 935–947.

Di Achille, G., Hynek, B.M., and Searls, M.L., 2009, Positive identification of lake strandlines in Shalbatana Vallis, Mars: Geophysical Research Letters, v. 36, L14201, doi: 10.1029/2009GL038854.

Duarte, C.M., Prairie, Y.T., Montes, C., Cole, J.J., Striegl, R., Melack, J., and Downing, J.A., 2008, CO_2 emissions from saline lakes: a global estimate of a surprisingly large flux: Journal of Geophysical Research, v. 113, G04041, doi: 10.1029/2007JG000637.

Dupraz, C., and Visscher, P.T., 2005, Microbial lithification in marine stromatolites and hypersaline mats: Trends in Microbiology, v. 13, p. 429–438.

Dupraz, C., Reid, P.R., Braissant, O., Decho, A., Norman, S.R., and Visscher, P.T., 2012, Processes of carbonate precipitation in modern microbial mats: Earth-Science Reviews, v. 96, p. 141–162.

Farías, M.E., Poiré, D.G., Arrouy, M.J., and Albarracin, V.E., 2011, Modern stromatolite ecosystems at alkaline and hypersaline high-altitude lakes in the Argentinean Puna, *in* Tewari, V., and Sekback, J., eds., Stromatolites: Interactions of Microbes with Sediments: Cellular Origin, Life in Extreme Habitats and Astrobiology, vol. 18: Springer, Dordrecht, Heidelberg, London, New York, p. 431–441.

Fernandez-Zenoff, V., Sineriz, F., and Farias, M.E., 2006, Diverse UV resistance of culturable bacterial community from high altitude wetland water: Current Microbiology, v. 52, p. 359–362.

Gao, Q., and Garcia-Pichel, F., 2011, Microbial ultraviolet sunscreens: Nature Reviews, Microbiology, v. 9, p. 791–802.

Garcia-Pichel, F., Al-Horani, F.A., Farmer, J.D., Ludwing, R., and Wade, B.D., 2004, Balance between microbial calcification and metazoan bioerosion in modern stromatolitic oncolites: Geobiology, v. 2, no. 1, p. 49–57.

Gasse, F., Fontes, J.Ch., Plaziat, J.C., Carbonel, P., Kacsmarska, I., De Deckker, P., Soulie-Marsche, I., Callot, Y., and Depeuble, P., 1987, Biological remains, geochemistry, and stable isotopes for the reconstruction of environmental and hydrological changes in the Holocene Lakes from North Sahara: Palaeogeography, Palaeoclimatology, Palaeoecology, v. 60, p. 1–46.

Golubic, S., Sergeev, V.N., and Knoll, A.H., 1995, Mesoproterozoic Archaeoellipsoides: akinetes of heterocystous cyanobacteria: Lethaia, v. 28, p. 285–298.

Goodwin, A.L., Michel, F.M., Phillips, B.L., Keen, D.A., Dove, M.T., and Reeder, R.J., 2010, Nanoporous structure and medium-range order in synthetic amorphous calcium carbonate: Chemistry of Materials, v. 22, p. 3197–3205.

Grotzinger, J.P., and Kasting, J.F., 1993, New constraints on Precambrian ocean composition: Journal of the Geological Society, v. 101, p. 235–243.

Grotzinger, J.P., and Knoll, A.H., 1999, Stromatolites in Precambrian carbonates; evolutionary mileposts or environmental dipsticks?: Annual Reviews in Earth and Planetary Sciences, v. 27, p. 313–358.

Grotzinger, J.P., and Rothman, D.H., 1996, An abiotic model for stromatolite morphogenesis: Nature, v. 383, p. 423–425.

Guido, A., Mastandrea, A., Demasi, F., Tosti, F., and Russo, F., 2012, Organic matter remains in the laminated microfabrics of the Kess-Kess mounds (Hamar Laghdad, Lower Devonian, Morocco): Sedimentary Geology, v. 263–264, p. 194–201.

Hagele, D., Leinfelder, R., Grau, J., Burmeister, E.G., and Struck, U., 2006, Oncoids from river Alz (southern Germany): tiny ecosystems in a phosphorous-limited environment: Palaeogeography, Palaeoclimatology, Palaeoecology, v. 237, p. 378–395.

Handley, K.M., Campbell, K.A., Mountain, B.W., and Browne, P.R.L., 2005, Abiotic-biotic controls on the origin and development of spicular sinter: *in situ* growth experiments, Champagne Pool, Waiotapu, New Zealand: Geobiology, v. 3, p. 93–114.

Handley, K.M., Turner, S.J., Campbell, K.A., and Mountain, B.W., 2008, Silicifying biofilm exopolymers on a hot-spring microstromatolite: templating nanometer-thick laminae: Astrobiology, v. 8, p. 747–770.

Heath, C., Leadbeater, B.C.S., and Callow, M.E., 1995, Effects of inhibitors on calcium carbonate deposition mediated by freshwater algae: Journal of Applied Phycology, v. 7, p. 367–380.

Jellison, R., Anderson, R., Melack, J.M., and Heil, D., 1996, Organic matter accumulation in sediments of hypersaline Mono Lake during a period of changing salinity: Limnology and Oceanography, v. 41, p. 1539–1544.

Jones, B., and Peng, X., 2012, Amorphous calcium carbonate associated with biofilms in hot spring deposits: Sedimentary Geology, v. 269–270, p. 58–68.

Jones, B., and Renault, R.W., 1994, Crystal fabrics and microbiota in large pisoliths from Laguna Pastos Grandes, Bolivia: Sedimentology, v. 41, p. 1171–1202.

Jordan, T., and Alonso, R., 1987, Cenozoic stratigraphy and basin tectonics of the Andes Mountains, 20°–28° South latitude: American Association of Petroleum Geologists (AAPG) Bulletin, v. 71, p. 49–64.

Kah, L.C., and Knoll, A.H., 1996, Microbenthic distribution of Proterozoic tidal flats: environmental and taphonomic considerations: Geology, v. 24, p. 79–82.

Kah, L.C., Lyons, T.W., and Chesley, J., 2001, Geochemistry of a 1.2 Ga carbonate-evaporite succession, northern Baffin and Bylot islands: implications for Mesoproterozoic marine evolution: Precambrian Research, v. 111, p. 203–234.

Kah, L.C., Bartley, J.K., Frank, T.D., and Lyons, T.W., 2006, Reconstructing sea-level change from the internal architectures of stromatolite reefs: an example from the Mesoproterozoic Sulky Formation, Dismal Lakes Group, arctic Canada: Canadian Journal of Earth Sciences, v. 43, p. 653–669.

Kah, L.C., Bartley, J.K., and Teala, D.A., 2012, Chemostratigraphy of the late Mesoproterozoic Atar Group, Taoudeni Basin, Mauritania: muted isotopic variability, facies correlation, and global isotopic trends: Precambrian Research, v. 200–203, p. 82–103.

Kalkowsky, E., 1908, Oolith und stromatolith in Norddeutchen Bund-sandstein: Deutsche Zeitschrift der Deutschen Geologischen Gesellschaft, v. 60, p. 68–125.

Kawaguchi, T., and Decho, A.W., 2002, Isolation and biochemical characterization of extracellular polymeric secretions (EPS) from modern soft marine stromatolites (Bahamas) and its inhibitory effect on $CaCO_3$ precipitation: Preparative Biochemistry and Biotechnology, v. 32, p. 51–63.

Kempe, J. and Kazmierczak, S., 2006, Genuine modern analogues of Precambrian stromatolites from caldera lakes of Niuafo'ou Island, Tonga: Naturwissenschaften, v. 93, p. 119–126.

Knoll, A.H., and Semikhatov, M.A., 1998, The genesis and time distribution of two distinctive Proterozoic stromatolitic microstructures: PALAIOS, v. 13, p. 408–422.

Knoll, A.H., Worndle, S., and Kah, L.C., 2013, Covariance of microfossil assemblages and microbialite textures across an upper Mesoproterozoic carbonate platform: PALAIOS, v. 28, p. 453–470.

Komatsu, G., Di Achille, G., Popa, C., Di Lorenzo, S., Rossi, A.P., and Rodriguez, J.A.P., 2009, Paleolakes, paleofloods, and depressions in Aurorae and Ophir plana, Mars; connectivity of surface and subsurface hydrological systems: Icarus, v. 201, p. 474–491.

Krammer, M., Velimirov, B., Fischer, U., Farnleitner, A.H., Herzig, A., and Kirschner, A.K., 2008, Growth response of soda lake bacterial communities to simulated rainfall: Microbial Ecology, v. 55, p. 194–211.

Li, H.-C., and Ku, T.,-L., 1997, $\delta^{13}C$-$\delta^{18}O$ covariance as a paleohydrological indicator for closed-basin lakes: Palaeogeography, Palaeoclimatology, Palaeoecology, v. 133, p. 69–80.

Lowenstein, T.K., and Risacher, F., 2009, Closed basin brine evolution and the influence of Ca–Cl inflow waters: Death Valley and Bristol Dry Lake California, Qaidam Basin, China, and Salar de Atacama, Chile: Aquatic Geochemistry, v. 15, p. 71–94.

Manzo, E., Perri, E., and Tucker, M.E., 2012, Carbonate deposition in a fluvial tufa system: processes and products (Corvino Valley—Southern Italy): Sedimentology, v. 59, p. 553–557.

Mcloughlin, N., Wilson, L.A., and Brasier, M.D., 2008, Growth of synthetic stromatolites and wrinkle structures in the absence of microbes: implications for the early fossil record: Geobiology, v. 6, p. 95–105.

Milana, J.P., 2009, Largest wind ripples on Earth?: Geology, v. 37, p. 343–346.

Monty, C.L.V., and Hardie, L.A., 1976, The geological significance of the freshwater blue-green algal calcareous marsh, *in* Walter, M.R., ed., Stromatolites: Developments in Sedimentology, vol. 20: Amsterdam,Elsevier, p. 447–477.

Morris, R.V., Ruff, S.W., Gellert, R., Ming, D.W., Arvidson, R.E., Clark, B.C., Golden, D.C., Siebach, K., Klingelhöfer, G., Schöder, C., Fleischer, I., Yen, A.S., and Squyres, S.W., 2010, Identification of carbonate-rich outcrops on Mars by the Spirit Rover: Science, v. 329, p. 421–424.

Murchie, S.L., Mustard, J.F., Ehlmann, B.L., Milliken, R.E., Bishop, J.L., Mkkeown, N.K., Noe Dobrea, E.Z., Seelos, F.P., Buczkowski, D.L., Wiseman, S.M., Arvidson, R.E., Wray, J.J., Swayze, G., Clark, R.N., Des Marais, D.J., Mcewen, A.S., and Bibring, J.P., 2009, A synthesis of Martian aqueous mineralogy after 1 Mars year of observations from the Mars Reconnaissance Orbiter: Journal of Geophysical Research, 114, E00D06, doi: 10.1029/2009JE003342.

Ordoñez, O.F., Flores, M.R., Dib, J.R., Paz, A., and Farías, M.E., 2009, Extremophile culture collection from Andean lakes: Extreme pristine environments that host a wide diversity of microorganisms with tolerance to UV radiation: Microbial Ecology, v. 58, p. 461–473.

Parkhurst, D.L., and Appelo, C.A.J., 1999, User's guide to PHREEQC (Version 2): a computer program for speciation, batch-reaction, one-dimensional transport, and inverse geochemical calculations: U.S. Geological Survey Water-Resources Investigations Report 99-4259, 312 p.

Pedley, M., 2000, Ambient Temperature Freshwater Microbial Tufas, *in* Riding, R.E. and Awramik, S.M., eds., Microbial Sediments, Springer, p. 179–186.

Perri, E., Manzo, E., and Tucker, M.E., 2012, Multi-scale study of the role of the biofilm in the formation of minerals and fabrics in calcareous tufa: Sedimentary Geology, v. 263–264, p. 16–29.

Politi, Y., Batchelor, D.R., Zaslansky, P., Chmelka, B.F., Weaver, J.C., Sagi, I., Weiner, S., and Addadi, L., 2010, Role of magnesium ion in the stabilization of biogenic amorphous calcium carbonate: a structure–function investigation: Chemistry of Materials, v. 22, p. 161–166.

Pope, M.C., and Grotzinger, J.P., 2000, Controls on fabric development and morphology of tufas and stromatolites Uppermost Pethei Group (1.8 Ga), Great Slave Lake, Northwest Canada, *in* Grotzinger, J.P., and James, N.P., Carbonate Sedimentation and Diagenesis in the Evolving Precambrian World: Society for Sedimentary Geology (SEPM) Special Publication 67, p. 103–121.

Pope, M.C., Grotzinger, J.P., and Schreiber, B.C., 2000, Evaporitic subtidal stromatolites produced by in situ precipitation: textures, facies associations and temporal significance: Journal of Sedimentary Research, v. 70, p. 1139–1151.

Purser, B.H., and., Loreau, J.P, 1973, Aragonitic supratidal encrustations on the Trucial Coast, Persian Gulf, *in* Purser, B.H., ed., The Persian Gulf, Holocene Carbonate Sedimentation in a Shallow Epeiric Continental Sea: New York, Springer, p. 343–376.

Reid, R.P., Visscher, P.T., Decho, A.W., Stolz, J.F., Bebout, B.M., Dupraz, C., Macintyre, I.G., Paerl, H.W., Pinckney, J.L., Prufert-Bebout, L., Steepe, T.F., and Des Marais, D.J., 2000, The role of microbes in accretion, lamination and early lithification of modern marine stromatolites: Nature, v. 406, p. 989–992.

Riding, R.E., 2000, Microbial carbonates: the geological record of calcified bacterial-algal mast and biofilms: Sedimentology, v. 47, Suppl. 1, p. 179–214.

Riding, R.E., 2008, Abiogenic, microbial and hybrid authigenic carbonate crusts: components of Precambrian stromatolites: Geologica Croatica, v. 6, no. 2–3, p. 73–103.

Riding, R.E., and Awramik, S.M., 2000, Microbial Sediments: Springer, Berlin, Heidelberg, New York, 331 p.

Risacher, F., and Eugster, H.P., 1979, Holocene pisolites and encrustations associated with spring-fed surface pools, Pastos Grandes, Bolivia: Sedimentology, v. 26, p. 253–270.

Risacher, F., and Fritz, B., 2009, Origin of salts and brine evolution of Bolivian and Chilean salars: Aquatic Geochemistry, v. 15, p. 123–157.

Risacher, F., Alonso, B., and Salazar, C., 2003, The origin of brines and salts in Chilean salars: a hydrochemical review: Earth-Science Reviews, v. 63, p. 249–293.

Rodriguez-Blanco, J.D., Shaw, S., and Benning, L.G., 2011, The kinetics and mechanisms of amorphous calcium carbonate (ACC) crystallization to calcite, via vaterite: Nano-scale, v. 3, p. 265–271.

Rouchy, J.M., Servant, M., Fournier, M., and Causse, C., 1996, Extensive carbonate algal bioherms in upper Pleistocene saline lakes of the central Altiplano of Bolivia: Sedimentology, v. 43, p. 973–993.

Seong Joo, L., and Golubic, S., 1999, Microfossil population in the context of synsedimentary micrite deposition and acicular carbonate precipitation: Mesoproterozoic Gaoyuzhuang Formation, China: Precambrian Research, v. 96, p. 183–208.

Seong Joo, L., and Golubic, S., 2000, Biological and mineral components of an ancient stromatolite: Gaoyuzhuang Formation, Mesoproterozoic of China, *in* Grotzinger, J.P., and James, N.P., Carbonate Sedimentation and Diagenesis in the Evolving Precambrian World: Society for Sedimentary Geology (SEPM) Special Publication 67, p. 91–102.

Sergeev, V.N., Knoll, A.H., and Grotzinger J.P., 1995, Paleobiology of the Mesoproterozoic Billyakh Group, Anabar Uplift, northeastern Siberia: Journal of Paleontology, v. 69, p. 1–37.

Shopov, Y.Y, 2004, Activators of luminescence in speleothems as source of major mistakes in interpretation of luminescent paleoclimatic records: International Journal of Speleology, v. 33, p. 25–33.

Singurindy, O., Berckowitz, B., and Lowell, R.P., 2004, Carbonate dissolution and precipitation in coastal environments: laboratory analysis and theoretical consideration: Water Resources Research, v. 40, W04401, doi: 10.1029/2003WR002651.

Stewart, P.S., 2003, Diffusion in biofilms: Journal of Bacteriology, v. 185, p. 1485–1491.

Summons, R.E., Amend, J.P., Bish, D., Buick, R., Cody, G.D., Des Marais, D.J., Dromart, G., Eigenbrode, J.F., Knoll, A.H., and Sumner, D.Y., 2011, Preservation of martian organic and environmental records: Final report of the Mars biosignature working group: Astrobiology, v. 11, p. 157–181, doi: 10.1089/ast.2010.0506.

Sumner, D.Y., 2004, Poor preservation potential of organics in Meridiani Planum hematite-bearing sedimentary rocks: Journal of Geophysical Research, v. 109, E12007, doi: 10.1029/2004JE002321.

Talbot, M.R., 1990, A review of the palaeohydrological interpretation of carbon and oxygen isotopic ratios in primary lacustrine carbonates: Chemical Geology (Isotope Section), v. 80, p. 261–279.

Talbot, M.R., and Kelts, K., 1990, Paleolimnological signatures from carbon and oxygen isotopic ration in carbonates from organic-carbon rich lacustrine sediments *in* Katz, B.J., Lacustrine Basin Exploration: Case Studies and Modern Analogs: American Association of Petroleum Geologists (AAPG) Memoir 50, p. 99–112.

Teske, A., and Stahl, D.A., 2002, Microbial mats and biofilms: evolution, structure and function of fixed microbial communities, *in* Staley, J.T., and Reysenbach, A.L., eds., Biodiversity of Microbial Life: Wiley-Liss, Inc., New York, p. 49–100.

Tosca, N.J., Knoll, A.H., and Mclennan, S.M., 2008, Water activity and the challenge of life on early Mars: Science, v. 320, p. 1204–1207.

Trichet, J., and Defárgue, C., 1995, Non-biologically supported organomineralization, *in* Allemand, D., and Cuif, J.P., eds., Proceedings 7th International Symposium on Biomineralization: Búlletin de l'Institute Océanographique de Monaco, v. 2, p. 203–236.

Valero-Garcés, B.L., Delgado-Huertas, A., Ratto, N., and Navas, A., 1999, Large ^{13}C enrichment in primary carbonate from Andean Altiplano lakes, northwest Argentina: Earth and Planetary Science Letters, v. 171, p. 253–266.

Valero-Garcés, B.L., Delgado-Huertas, A., Ratto, N., and Navas, A., and Edwards, L., 2000, Paleohydrology of Andean saline lakes from sedimentological and isotopic records, Northwestern Argentina: Journal of Paleolimnology, v. 24, p. 343–359.

Vandervoort, D.S., Jordan, T.E., Zeitler P.K., and Alonso, R.N., 1995, Chronology of internal drainage development and uplift, southern Puna plateau, Argentine Central Andes: Geology, v. 23, p. 145–148.

Vasconcelos, C., Mckenzie, J.A., Bernasconi, S., Grujic, D., and Tien, A.J., 1995, Microbial mediation as a possible mechanism for natural dolomite formation at low temperatures: Nature, v. 377, p. 220–222.

Visscher, P.T., and Stolz, J.F., 2005, Microbial mats as bioreactors: populations, processes and products: Palaeogeography, Palaeoclimatology, Palaeoecology, v. 219, p. 87–100.

Visscher, P.T., Reid, R.P., and Bebout, B.M., 2000, Microscale observations of sulfate reduction: correlation of microbial activity with lithified micritic lamina in modern stromatolites: Geology, v. 28, no. 10, p. 919–922.

Vuille, M., and Amman, C., 1996, Regional snowfall patterns in the high arid Andes: Climate Change, v. 36, p. 413–423.

Wade, B.D., and Garcia-Pichel, F., 2003, Evaluation of DNA extraction methods for molecular analyses of microbial communities in modern calcareous microbialites: Geomicrobiology Journal, v. 20, no. 6, p. 549–561.

Walter, M.R., 1972, Stromatolites and biostratigraphy of the Australian Precambrian and Cambrian: Special Papers in Palaeontology, v. 11, p. 1–190.

Winsborough, B.M., 2000, Diatoms and benthic microbial carbonates, *in* Riding, R.E., and Awramik, S.M., eds., Microbial Sediments: Springer, Berlin, Heidelberg, New York, p. 76–83.

Winsborough, B.M., and Golubic, S., 1987, The role of diatoms in stromatolite growth: two examples from modern freshwater settings: Journal of Phycology, v. 23, p. 195–201.

Winsborough, B.M., Seeler, J.S., Golubic, S., Folk, R.L., and Maguire, B., 1994, Recent fresh-water lacustrine stromatolites, stromatolitic mats and oncoids from northeastern Mexico, *in* Bertrand-Sarfati, J., and Monty, C., eds., Phanerozoic Stromatolites II: Dordrecht, Kluwer, p. 71–100.

Wotton, R.S., 2004, The ubiquity and many roles of exopolymers (EPS) in aquatic systems: Scientia Marina, v. 68, p. 13–21.

Zavarzin, G.A., Orleanskii, V.K., Gerasimentko, L.M., Pushko, S.N., and Ushatinskaya, G.T., 2003, Laboratory simulation of cyanobacterial microbial mats and the alkaline geochemical barrier: Microbiology, v. 72, p. 80–85.

Received 10 October 2013; accepted 26 June 2014.